

INVISCID FLOW CALCULATION AROUND A FLEXIBLE AIRSHIP

Kamal El Omari, Eric Schall,
Bruno Koobus and Alain Dervieux

Abstract. In the context of an airship development programme, inviscid flow behavior and its coupling with structure flexibility are investigated. For this purpose, we have chosen a nonlinear analysis tool relying on the unsteady Euler model for the flow part and the classical elastodynamic equations for the structure. The numerical model for the flow is based on a Mixed Element Volume discretization derived in an Arbitrary-Lagrangian-Eulerian framework in order to cope with the structural deformations. The case of low-Mach flows (natural flight regime for an airship) can be handled by a special dissipation preconditioner which improves the accuracy of the flow simulation. The structural model, coupled to the flow solver, is discretized by the finite element method in a Lagrangian formulation. In this work we have performed a series of inviscid flow calculations with the goal to evaluate accurately the global aerodynamical coefficients. We first compare the influence of different stiffeners in the airship structural model for flows with zero and non-zero (20°) angle of attack. Then, we study the influence of the numerical dissipation and of the low-Mach preconditioning. We observe –as expected– the stabilizing effect of the stiffeners, specially longitudinal ones. The positive impact of low Mach preconditioning and numerical dissipation on the results is also evaluated.

Keywords: Inviscid Flow, Arbitrary-Lagrangian-Eulerian, Fluid-Structure Interaction, Unstructured Deformable Mesh, Prolate Spheroid

AMS classification:

§1. Introduction

The existing projects for airships are generally characterized by two particular Computational Fluid Dynamics (CFD) features:

- the necessity to be less heavy than air leads to some flexibility of the whole frame,
- this flexibility induces deformations that can be at term amplified by the very unequal weight repartition (useful load versus lifting volume).

In the context of an airship development programme, we need to simulate the complete behavior of an airship in real flow conditions and to take into account the hull deformations specially for flows with high angle of attack. In the scope of this first study we neglect, as a first approximation, the effect of fluid viscosity and of the turbulent character of the flow. These aspects are the subject of an independent study [1]. These simplifications make possible to use coarser meshes and to run the many calculations required by a parametric study. Hence, we have chosen a nonlinear analysis tool [2][3][4][5][6][7] relying on the unsteady inviscid Euler model for the flow part and the classical elastodynamic equations for the structure. The flow solver is based on a Mixed Element Volume discretization derived in an Arbitrary-Lagrangian-Eulerian (ALE) framework in order to cope with the structural deformations. The accuracy of low-Mach flows simulations (natural flight regime for an airship) can be enhanced by a special dissipation preconditioner (Tukel preconditioner) [8]. The structural model, coupled to the flow solver, is discretized by the finite element method in a Lagrangian formulation. In order to perform a generic study at this early stage of our airship development project, we have chosen to use a generic geometry. Hence, we choose to study a flow around a prolate spheroid 6 : 1 structure. This geometry is quite close to an airship geometry and has been widely experimentally studied [9]. The same geometry is also used for our previously cited viscous turbulent study [1].

§2. Formulation of transient nonlinear aeroelastic problems

The problem of the motion of the fluid/structure interface that occurs in coupled aeroelastic problems is addressed by solving the fluid equations on deformable dynamic meshes. An Arbitrary Lagrangian Eulerian (ALE) formulation is used in order to perform the integration of the fluid equations on a moving mesh. The coupled aeroelastic problem to be solved can then be viewed as a three-field problem [3]: the fluid, the structure and the dynamic mesh which is represented by a pseudo-structural system. The semi-discrete equations governing the three-way coupled problem can be written as follows

$$\begin{aligned} \frac{\partial}{\partial t}(V(x, t)w(t)) + F^c(w(t), x, \dot{x}) &= R(w(t), x) \\ M \frac{\partial^2 q}{\partial t^2} + f^{int}(q) &= f^{ext}(w(t), x) \\ \tilde{M} \frac{\partial^2 x}{\partial t^2} + \tilde{D} \frac{\partial x}{\partial t} + \tilde{K}x &= K_c q \end{aligned} \quad (1)$$

where t designates time, x the position of a moving fluid grid point, w is the fluid state vector, V results from the finite element/volume discretization of the fluid equations, F^c is the vector of convective ALE fluxes, R is the vector of diffusive fluxes, q is the structural displacement vector, f^{int} denotes the vector of internal forces in the structure, f^{ext} the vector of external forces, M is the finite element mass matrix of the structure, \tilde{M} , \tilde{D} and \tilde{K} are fictitious mass, damping and stiffness matrices associated with the moving fluid grid and K_c is a transfer matrix that describes the action of the motion of the structural side of the fluid/structure interface on the fluid dynamic mesh.

§3. Numerical methodology for solving coupled nonlinear aeroelastic problems

In this section, we give the main features of the numerical methods employed in this work for solving the coupled nonlinear aeroelastic problem given by Eqs. (1). For more details, the reader is invited to examine the references given in the text.

3.1. Discretization of transient nonlinear aeroelastic problems

- **Spatial discretization**

The spatial discretization of the fluid equations is based on a Mixed Element Volume formulation on unstructured meshes. It combines a Roe's upwind scheme for computing the convective fluxes, and a Galerkin centered method for evaluating the viscous terms. Second-order space accuracy is achieved through a piecewise linear interpolation method based on the MUSCL (Monotonic Upwind Scheme for Conservation Laws) procedure [10, 11]. Since we are considering subsonic flows, the shock capturing facilities are inhibited in the flow solver ("no limiter"). Moreover, in order to obtain a low level of numerical dissipation, a scalar coefficient γ is used to weight the numerical viscosity introduced by the Roe's approximate Riemann solver (L stands for left, and R for right):

$$\begin{aligned} \Phi(W_L, W_R, n) = & 0.5 (F^c(W_L) + F^c(W_R)) \cdot n \\ & - 0.5 \gamma |J|(W_R - W_L) \end{aligned} \quad (2)$$

in which Φ denotes Roe's numerical flux, n is the normal vector to cell boundary and J the Jacobian of the ALE convective fluxes F^c times the normal n . Usual option is $\gamma = 1$ for standard Roe's solver, and for lower values of numerical viscosity, smaller values of γ will be preferred. Since the global flow is characterized by a medium-small Mach number, we found useful to compare Roe's scheme and its Turkel's preconditioned variant for low Mach flows. The description of this feature is out of the scope of this paper and we refer for example to [8].

For addressing the problem of flow simulations on moving grids, an ALE formulation is incorporated in the flow solver. The numerical algorithms used with this ALE formulation satisfy the Geometric Conservation Laws (GCL) [12, 13] that govern flow computations on moving grids.

The structure is represented by a finite element model, and its dynamics behavior is predicted using the true displacement, velocity and acceleration degrees of freedom.

At selective time-steps of an aeroelastic simulation, the dynamic fluid mesh is updated to conform the most recently computed configuration of the structure. The points lying on the fluid/structure boundary are first adjusted to conform to the new position of the surface of the structure, then the remainder of the fluid grid points are repositioned accordingly. In the methodology used in this work, the new position of the interior grid

points is determined from the displacement solution of a discrete pseudo-structural problem representing the unstructured dynamic fluid mesh. The pseudo-structural system is constructed by lumping a fictitious mass at each vertex of the fluid mesh and attaching fictitious lineal springs to each edge connecting two vertices [3]. In order to enforce the robustness of this method based on lineal springs, torsional springs can be added [6]. This discrete system is represented by the third of Eqs. (1) where $\tilde{M} = \tilde{D} = 0$.

Finally, in fluid/structure interaction problems the fluid and structure meshes have often non-matching discrete interfaces. In that case, we use the load and motion transfer algorithms described in [14] for evaluating properly the pressure forces on the surface of the structure, and transferring correctly the structural motion to the fluid mesh. In particular, the loads induced by the fluid on the structure are computed in a conservative way.

- **Time discretization**

For solving accurately and efficiently the flow equations given by the first of Eqs. (1) on dynamic meshes, a second-order time-accurate implicit algorithm preserving the GCL [7] is employed. The time discretization is based on a second-order backward difference scheme. The nonlinear flow equations derived from the time-discretization are solved by a defect-correction (Newton-like) method [15].

The structural equations of dynamic equilibrium given by the second of Eqs. (1) are solved with a second-order time-accurate implicit scheme where the trapezoidal method is used.

3.2. Staggered solution procedure

The solution of the coupled fluid/structure problem (1) is computed by a staggered solution procedure in the time domain [16]. More precisely, we use the staggered algorithm given in [17] which satisfies the GCL as well as the continuity of both the displacement and velocity fields at the fluid/structure interface. This algorithm can be written as follows

1. Using the mesh position $x^{n-\frac{1}{2}}$, and the mesh velocity \dot{x}^n that matches the structural velocity \dot{q}^n on the fluid/structure interface, update the mesh coordinates as follows

$$x^{n+\frac{1}{2}} = x^{n-\frac{1}{2}} + \Delta t \dot{x}^n$$

2. Using $x^{n-\frac{1}{2}}$, $x^{n+\frac{1}{2}}$ and \dot{x}^n , update the fluid state vector $w^{n+\frac{1}{2}}$ in a manner that satisfies the GCL
3. Using the pressure computed from $w^{n+\frac{1}{2}}$, compute q^{n+1} and \dot{q}^{n+1} using the midpoint rule.

§4. Test-case

4.1. Structural characteristics

The geometry studied here is the prolate spheroid 6 : 1 of length $L = 1.37\text{ m}$. This structure consists of a relatively flexible hull with two extremities made with a harder material; this is the first investigated configuration of the structure. In a second structure, we add three annular stiffeners to the flexible hull, formed by hard tubes (second studied configuration). Finally, a third structure is defined by adding to the previous configuration four longitudinal stiffeners made of the same material as the previous ones. We give in Tab. 1 the characteristics of the different materials used in the structure. A sketch of the prolate with annular and longitudinal stiffeners is shown in Fig. 1. The flexible hull and the hard extremities are modeled by triangular shell elements, and are discretized by 2274 nodes and 4544 triangles (Fig. 2). The stiffeners are modeled by beam elements with $2.76 \times 10^{-4}\text{ m}^2$ as sectional area, their three moments of inertia are 2.36×10^{-7} , 1.18×10^{-7} and 1.18×10^{-7} . The structure is fixed at its back.

	e	E	ν	ρ
<i>Extremities</i>	0.02	1×10^{12}	0.3	3500
<i>Hull</i>	0.005	1×10^9	0.3	3500
<i>Stiffeners</i>		7×10^{10}	0.3	8800

Table 1: Characteristics of different materials used in the prolate structure, e : Thickness, E : Young’s modulus, ν : Poisson’s coefficient, ρ : density, (IS units).

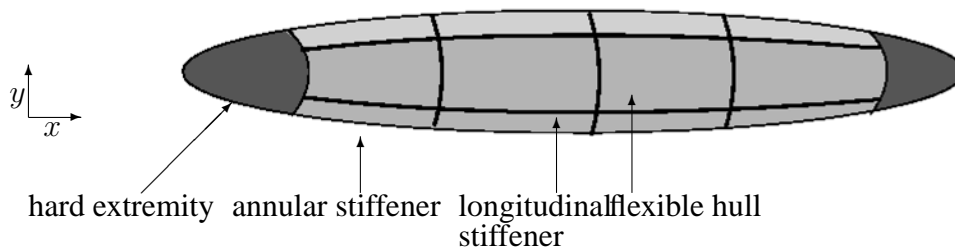


Figure 1: Prolate structure and stiffeners position

The first four eigen-modes of each structural model is given by: a bending mode, a buckling mode, a mix of two bending modes, and finally a stretching mode.

The first four eigenfrequencies of the previous structural models are given in Tab. 2.

4.2. Flow conditions and numerical issues

The free-stream flow conditions are: Mach number $M_\infty = 0.15$, pressure $P_\infty = 1.013 \times 10^5\text{ Pa}$ and density $\rho = 1.1\text{ kg m}^{-3}$. The angle of attack is set to 0° or 20° .

	Struct. 1	Struct. 2	Struct. 3
<i>freq. 1</i>	11.2	14.7	32
<i>freq. 2</i>	61.2	88	131.1
<i>freq. 3</i>	70.5	94.2	191.4
<i>freq. 4</i>	109.5	161.9	394.7

Table 2: Eigenfrequencies associated to the three investigated structural models (Hz).

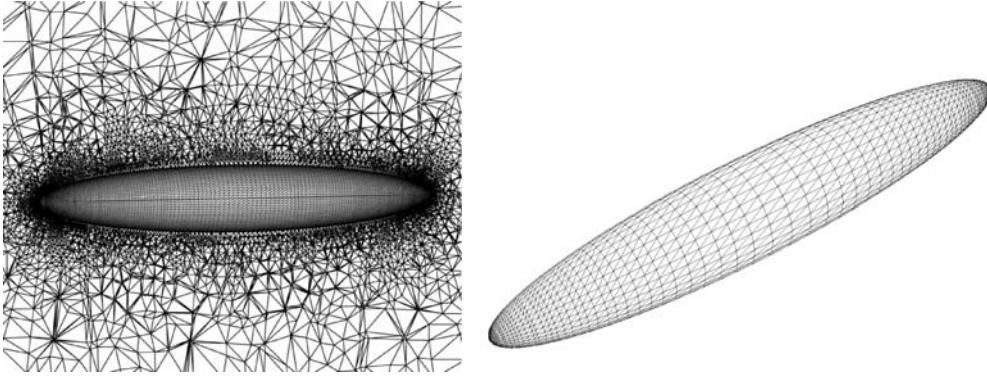


Figure 2: Fluid (left) and structure (right) meshes

The fluid mesh contains 50018 vertices and 264426 tetrahedra (Fig. 2) and does not match with the structural one at the prolate surface.

The fluid model is the Euler equations. Unless mentioned otherwise, the calculations are performed with a coefficient of numerical viscosity lowered to $\gamma = 0.3$ and Roe's scheme with Turkel's preconditioning. The structure calculations are damped [5] for a faster convergence of the coupled solution.

The fluid mesh is decomposed into 10 subdomains to achieve parallel computations, and the coupled fluid-structure calculations are performed on 11 processors since one processor is allocated for the structural solver.

§5. Results

We have first performed inviscid steady solutions around the prolate with the flow solver alone. Figs. 3 show the Mach number isolines for 0 and 20° angle of attack. In a second step, we have performed the computations of static fluid-structure coupling with the different structural models of the generic airship described in Section 4. Structure deformations that result from the interaction with these inviscid low speed flows are given in Figs. 4. These pictures represent the shape of the structure when the stationary solution of the coupled problem is reached. We compare in this figure the effect of the angle of attack and the influence of the three different configurations of stiffeners on the static coupling. The structure deformations are graphically amplified 100 times for better visibility. We notice first that a flow with zero angle of attack results in less important deformations, so that the effect of the stiffeners remains minor compared to the 20° angle of attack case. For this last case, we observe two main deformations:

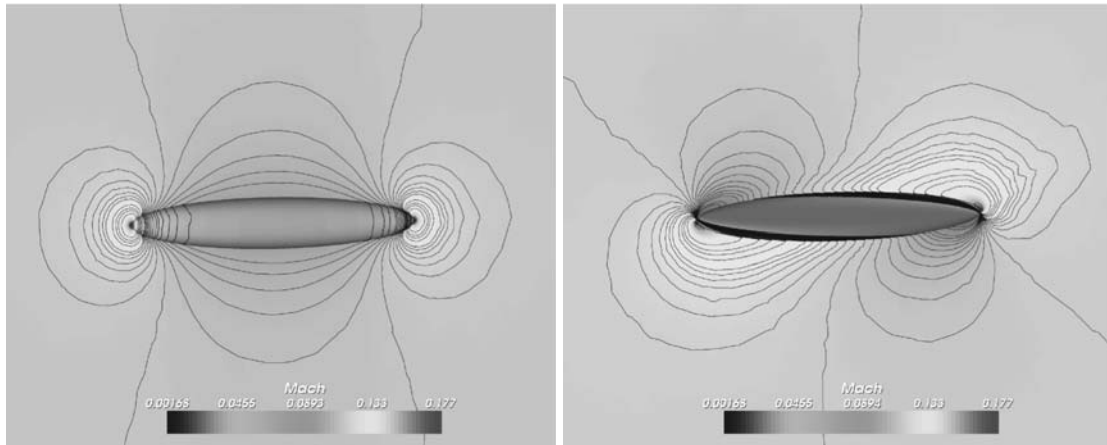


Figure 3: Contours of Mach number for 0 (left) and 20° (right) angle of attack

a flexion of the structure in the flow direction and a flattening of the flexible part of the structure. The latter deformation is avoided by adding annular stiffeners, and the former one by the longitudinal stiffeners. As mentioned before, we are looking for the stationary solution of

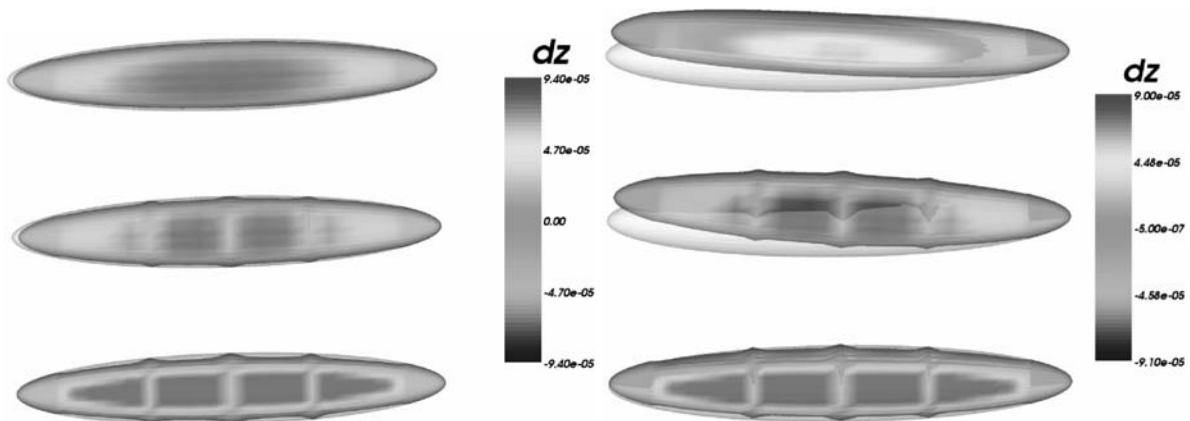


Figure 4: Structure deformation obtained for a static coupling with 0 (left) and 20° (right) angle of attack. The stiffeners are added from top to bottom of the figures. The deformations are amplified 100 times. Colours indicate the intensity of the cross-deformations (m).

the coupled problem by adequately damping the structure. So, to give an idea of the solution evolution with time, we plot in Figs. 5 the vertical displacement (on y direction, see Fig. 1) of the nose of the prolate as well as the lift coefficient for the three investigated structural models. We notice in these pictures the important acceleration role of the stiffeners in the stabilization of the structure: the harder the structure is, the faster the static coupled solution is reached.

We give in Tab. 3 the stabilized aerodynamic coefficients C_x and C_y obtained with the different angles of attack and structural models. We also present the results obtained by changing the amount of numerical viscosity through the scalar coefficient γ and by removing low Mach Turkel's preconditioning. The reference surfaces used for the evaluation of C_x and C_y are respectively $S_x = \pi(L/12)^2$ and $S_y = \pi L^2/24$. In this table we can notice that the stiffeners

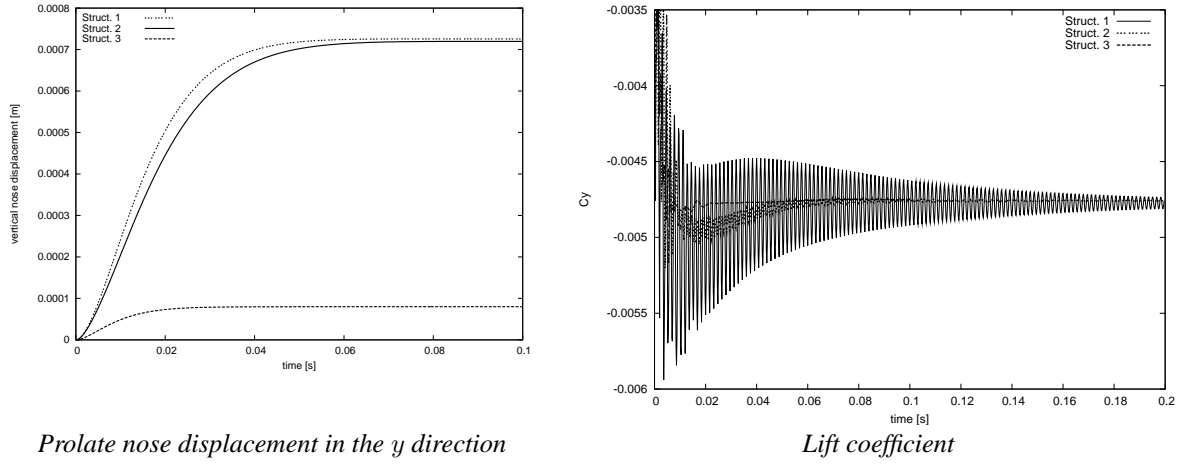


Figure 5: Evolution of vertical displacements and lift coefficient versus time for the three structural models with a flow at 20° angle of attack.

does not change the values of the computed aerodynamical coefficients: the displacement of the structure was not so important. On the other hand, we observe that increasing the numerical viscosity modifies noticeably the aerodynamic results as well as removing the low Mach preconditioning. We confirm here the positive impact of Turkel's preconditioning for such low Mach number flow simulations.

Angle of attack	C_x	C_y
Structure 1		
0° , $\gamma = 0.3$, Turkel	0.001332	0.0000025
20° , $\gamma = 0.3$, Turkel	0.002189	0.0047615
20° , $\gamma = 1$, Turkel	0.004003	0.0128703
20° , no Turkel	0.004867	0.0138653
Structure 2, $\gamma = 0.3$, Turkel		
0°	0.001332	0.0000024
20°	0.002175	0.0047580
Structure 3, $\gamma = 0.3$, Turkel		
0°	0.001236	0.000003
20°	0.002178	0.004751

Table 3: Aerodynamic coefficients

§6. Conclusion

In this work, we have investigated in an ALE framework the fluid-structure interaction of a flexible prolate spheroid in inviscid flows with and without angle of attack. We have studied the effect of two types of stiffeners: annular and longitudinal ones. According to the static fluid-structure coupled simulations performed, we notice, as expected, that the longitudinal

stiffeners limit the flexion of the prolate, and annular ones prevent the prolate from flattening. We have also investigated the influence of some numerical aspects: large numerical viscosity alters considerably the aerodynamical results, and low Mach preconditioning of the numerical viscosity improves the simulation accuracy for relatively low speed flows as those encountered around airships in flight. This study is a first step in a global investigation concerning flows around flexible airship hulls, and it introduces the next investigations based on finer grids and viscous turbulent models.

Acknowledgements

The authors are grateful to *Conseil Régional d'Aquitaine* for its financial support to the scientific airship project of Pau University and thank the Centre Informatique National de l'Enseignement Supérieur (CINES) for providing the computational resources.

References

- [1] K. EL OMARI, E. SCHALL, B. KOOBUS AND A. DERVIEUX. Turbulence Modeling Challenges in Airship CFD Studies, *this issue*.
- [2] B. KOOBUS, C. FARHAT. AND H. TRAN, Computation of unsteady viscous flows around moving bodies using the $k-\varepsilon$ turbulent model on unstructured dynamic grids. *Comput. Methods Appl. Mech. Engrg.*, 190 (2000), 1441-1466.
- [3] C. FARHAT, High Performance Simulation of Coupled non-linear Transient Aeroelastic Problems, *AGARD Report R-807, Special Course on Parallel Computing in CFD, North Atlantic Treaty Organization (NATO)*, October 1995.
- [4] A. DERVIEUX (ed.) *Fluid-Structure Interaction, Revue Européenne des Eléments Finis*, 9,6-7, Hermes, 2000
- [5] R. LARDAT, B. KOOBUS, F. RUFFINO, C. FARHAT AND A. DERVIEUX. Premières investigations du couplage fluide-structure autour d'un lanceur spatial générique, *Rapport de recherche INRIA*, N° 4314, (2001).
- [6] C. FARHAT, C. DEGAND, B. KOOBUS AND M. LESOINNE. Torsional Springs for Two-Dimensional Dynamic Unstructured Fluid Meshes, *Computer Methods in Applied Mechanics and Engineering*, 163, (1998), 231-245.
- [7] B. KOOBUS AND C. FARHAT. Second-Order Time-Accurate and Geometrically Conservative Implicit Schemes for Flow Computations on Unstructured Dynamic Meshes, *Computer Methods in Applied Mechanics and Engineering*, 170, (1999), 103-130.
- [8] E. SCHALL, C. VIOZAT, B. KOOBUS AND A. DERVIEUX. Computation of Low Mach Thermal Flows with Implicit Upwind Methods, *International Journal of Heat and Mass Transfer*, 46, 20 (2003), 3909-3926.
- [9] C.J. CHESNAKAS AND R.L. SIMPSON. A Detailed Investigation of the 3-D Separation about a 6:1 Prolate Spheroid at Angle of Attack, *AIAA Journal*, 35, 6 (1997), 990-999.
- [10] B. VAN LEER. Towards the Ultimate Conservative Difference Scheme V: a Second-Order Sequel to Godunov's Method, *J. Comp. Phys.* (1979), 32:361-370.

- [11] A. DERVIEUX. Steady Euler Simulations Using Unstructured Meshes, *Von Karman Institute Lecture Series* (1985.)
- [12] M. LESOINNE AND C. FARHAT. Geometric Conservation Laws for Aeroelastic Computations Using Unstructured Dynamic Meshes, *AIAA Paper 95-1709*, 12th AIAA Computational Fluid Dynamics Conferenc (1995), San Diego, CA.
- [13] B. NKONGA AND H. GUILLARD. Godunov Type Methods on Non-Structured Meshes for Three-Dimensional Moving Boundary Problems, *Comp. Methods Appl. Mech. Engrg.* 113 (1994) 183-204.
- [14] C. FARHAT, M. LESOINNE AND P. LE TALLEC. Load and Motion Transfer Algorithms for Fluid/Structure Interaction problems with Non-Matching Discrete Interfaces: Momentum and Energy Conservation, Optimal Discretization and Application to Aeroelasticity, *Computer Methods in Applied Mechanics and Engineering*, 157, (1998), 95-114.
- [15] R. MARTIN AND H. GUILLARD. A Second-Order Defect Correction Scheme for Unsteady Problems, *Comput. and Fluids*, (1996), 25:9-27.
- [16] C. FARHAT, M. LESOINNE AND N. MAMAN. Mixed Explicit/Implicit Time Integration of Coupled Aeroelastic Problems: Three-Field Formulation, Geometric Conservation and Distributed Solution, *Internat. J. Numer. Meths. Fluids*, 21 (1995), 807-835.
- [17] C. FARHAT AND M. LESOINNE, On the accuracy, stability and performance of the solution of three-dimensional nonlinear transient aeroelastic problems by partitioned procedures, *AIAA Paper 96-1388*, 37th AIAA/ASME/ASCE/AHS /ASC Structures, Structural Dynamics and Materials Conference, (1996), Salt Lake City, UT.

K. El Omari and E. Schall

IUT GTE, UPPA

1 Av. de l'Université

64000 Pau

kamal.elomari@univ-pau.fr and eric.schall@univ-pau.fr

B. Koobus

Université de Montpellier II

Place Eugène Bataillon, dépt. Math.

CC 051, F-34095 Montpellier Cedex 5

koobus@darboux.math.univ-

montp2.fr

A. Dervieux

INRIA, 2003 Route des Lucioles

F-06902 Sophia-Antiplolis Cedex

alain.dervieux@inria.fr